



## Research Article

# Exergetic performance analysis and comparison of oxy-combustion and conventional gas turbine power cycles

Ibrahim OZSARI<sup>1,\*</sup>, Yasin UST<sup>2</sup>, Asim Sinan KARAKURT<sup>2</sup>

<sup>1</sup>Department of Naval Architecture and Marine Engineering, Bursa Technical University, Yildirim, Bursa, 16350, Türkiye

<sup>2</sup>Department of Naval Architecture and Marine Engineering, Yıldız Technical University, Besiktas, İstanbul, 34349, Türkiye

## ARTICLE INFO

### Article history

Received: 22 January 2022

Revised: 04 April 2022

Accepted: 06 June 2022

### Keywords:

Thermodynamic Analysis;  
Oxy-Combustion Cycle; Clean  
Energy ECOP; EFECPOD;  
Exergy Density

## ABSTRACT

Oxy-combustion technologies are green energy systems and an impressive solution to climate change and global warming. This study presents a detailed exergy analysis obtained for oxy-combustion power systems in comparison with a conventional gas turbine power system. The results include net power, overall thermal efficiency, exergy destruction, exergy efficiency, power density, exergetic performance coefficient (EPC), ecological performance coefficient (ECOP), effective ecological power density (EFECPOD), and mean exergy density (MED), and cost of power density (COPD), which are calculated as functions of pressure and oxygen ratios. The conventional gas turbine power system obtained a pressure ratio for maximum net power of 20.8. Similarly, oxy-combustion power cycles at 26%, 28%, and 30% oxygen ratios have respective pressure ratios for maximum net power of 23.3, 27.4, and 29.7. Results from 24%-30% oxygen ratios are displayed to show the reactant oxygen's effect on the oxy-combustion power cycles. Increases in the pressure ratio show decreases in the total exergy destruction in both the conventional gas turbine power system and the oxy-combustion power systems. Meanwhile, increases in the pressure ratio show increases in the total efficiency, power density, exergy efficiency, EPC, EFECPOD, and MED in both the conventional gas turbine and the oxy-combustion power systems. In addition, increases in the oxygen ratio in the oxy-combustion power systems show different characteristics for these parameters based on the pressure ratio of the cycle. In terms of COPD, conventional gas turbine power systems are more advantageous than oxy-combustion power systems. Optimum COPD is obtained at a pressure ratio of 25.6.

**Cite this article as:** Ozsari I, Ust Y, Karakurt AS. Exergetic performance analysis and comparison of oxy-combustion and conventional gas turbine power cycles. Sigma J Eng Nat Sci 2023;41(3):575–591.

## INTRODUCTION

As in the past, the most important tools needed in modern times for sustaining life are undoubtedly fire, air, soil, and water. Energy is a magnitude preserved in the universe

based on these four elements. In other words, when we produce energy using any source, we reveal the substances that exist in it and interact with other. [1] Fossil fuels have been came into our lives as the primary energy production

### \*Corresponding author.

\*E-mail address: [Ibrahim.ozsari@btu.edu.tr](mailto:Ibrahim.ozsari@btu.edu.tr)

This paper was recommended for publication in revised form by Editor Abdelraheem Mahmoud Aly



source alongside the Industrial Revolution and are among the most frequently used resources for meeting the ever-increasing energy needs of today. According to data from the International Energy Agency, the ever-increasing global amount of CO<sub>2</sub> is a major problem, despite decreasing from 33.4 GT (gigatonnes) to 31.5 GT from 2019 to 2020 due to the decreases in movement and industrial production from the COVID-19 pandemic [2]. More environmentally friendly and efficient systems are being designed with the developments in technology, but thousands of energy production facilities still use older technologies that have both negative effects on the environment and work inefficiently. One of the technologies that will provide this is Carbon Capture Utilization and Storage (CCUS) systems [3]. The captured CO<sub>2</sub> can be transported as compressed gas or liquefied. Although both natural and human-built areas are used for storage purposes, storage in salt water aquifers is more appropriate in terms of both cost and ecology [4]. The released or stored CO<sub>2</sub> is generally used in places such as refrigeration plants or the food industry [5]. Carbon capture processes and technologies can be generally evaluated in three classes. [6]. In addition to the practice of these three methods, capture and membrane separation carbon capture technologies are also found using solvents, sorbents, cooling, chemical cycles, and biological organisms [7].

Oxy-fuel combustion processes can be applied in metal, glass, and ceramic production facilities as well as incineration plants and thermal power plants, which generally supply higher heat and power needs [8]. In oxy-fuel combustion processes, the normal air supplied to the system in the combustion chamber is replaced by oxygen-enriched air with a higher O<sub>2</sub> concentration. The concentration of CO<sub>2</sub> increases in the gases released as a result of the oxy-fuel combustion, and even if used with pure O<sub>2</sub>, only CO<sub>2</sub> and H<sub>2</sub>O are produced. In this way, the intense CO<sub>2</sub> released can be easily captured and stored [9]. A large proportion or even complete capture of the produced CO<sub>2</sub> allows CCUS systems to operate more efficiently and economically. Increasing the concentration of oxygen also increases NO and SO<sub>2</sub> emissions while reducing unburnt fuel as well as carbon monoxide (CO) and NO<sub>2</sub> emissions. High oxygen content also improves the combustion efficiency for both combustion atmospheres [10].

In addition to these, CCUS has many advantages such as reducing fuel costs while increasing plant efficiency, enabling other harmful particles to be filtered with modifications, being competitive compared to other carbon capture technologies, and having a smaller combustion chamber compared to air combustion [11]. Despite the advantages mentioned above, CCUS has disadvantages such as higher investment and operating costs, constraints of storage conditions, difficulties in transporting the stored CO<sub>2</sub>, failure to ensure sustainability in CO<sub>2</sub> supply, and non-continuous regional policies that have prevented its application from spreading [12].

In this context, many articles, papers, reports, and patents are found related to carbon capture technologies and oxy-fuel combustion processes. According to Scopus data, 2,880 studies have been conducted under the topic of oxy-combustion, with the trend increasing between 1985–2021; oxy-combustion has also received more than 40,000 references.

Maximizing the thermal efficiency or power produced in thermal systems is neither a sufficient nor realistic criterion on its own. The reason for this is the uncertainty of the size or dimension of the thermal system providing the demanded power or thermal load. For this reason, evaluating a thermal systems by including the produced power and thermal efficiency specifications as well as the dimensions of the system in the objective functions will provide more realistic approaches. For this purpose, Sahin et al. [13] has proposed the power density criteria addressing the system dimensions and performance within the constraints of the first law of thermodynamics and defined as the ratio of the power generated to the maximum volume in a Brayton cycle. However, optimization indicative of the maximization of this function have been performed for such power cycles as the Carnot [14–16], Brayton [17–21], dual [22,23], Atkinson [24,25], and diesel [26] systems in recent years. Studies have investigated the effects design and irreversibility parameters have on performance criteria. In general, the obtained results were compared with the data under maximum power conditions, which show the maximum power density conditions to be more advantageous in terms of efficiency and size. As a result, more applicable results can be obtained when the advantages, disadvantages, and investment costs are considered together.

The exergetic performance criterion (EPC) provides information on how a system or component utilizes its useful work potential or exergy and is defined as the total exergy output per unit loss rate. The aim is to have the EPC value in a power cycle or a component be at its maximum. In this context, EPC analyses have been carried out for regenerative gas turbine cogeneration [27], dual-cycle cogeneration [28] and dual-Miller cycle cogeneration [29] systems that take irreversibilities or losses into account. In general, the results show the conditions where the EPC value is at its maximum to be more advantageous in terms of entropy production rate, exergy efficiency, and initial investment cost while having lower exergy output than the maximum values of the dimensionless ecological function and the dimensionless total exergy output. Along with power cycles and their components, EPC has also been applied to different types of refrigeration cycles [30–33].

The ecological performance coefficient (ECOP) criterion, which uses the outputs of both the first and the second laws of thermodynamics together and provides information about both the performance and the ecological effects of the system, is another important criterion this study examines. Ust [34–36] proposed the objective

function as being the power generated per entropy generation in heat engines instead of as an ecological function [37]. Many optimization studies have been carried out using the ECOP criterion, some of which are given below. In this context, many optimization studies have been carried out for Otto [38], Carnot [39], diesel with various modifications [40–42], dual [43], dual-Atkinson [44], Braysson [45], organic Rankine [46], Ericsson [47], and Brayton power cycles with different characteristics [48–53] that take the losses and irreversibilities in the system into account. These studies are generally conducted as parametric studies according to the design and irreversibility parameters of the cycles. The literature shows the applicability of ECOP to have been examined and the results compared with those from the maximum power output criterion as well as other ecological performance criteria. The results show significant advantages to have been achieved in terms of entropy generation and thermal efficiency in cycles operating under maximum ECOP conditions albeit with some decrease in power output. The applications of the ECOP criterion as well as power cycles for ideal and real refrigeration cycles [54–60] and heat pumps with different numbers of source temperatures [61–63] have been brought to the literature.

Another important criterion describing the relationship between size and power output is the effective ecological power density criterion (EFECPOD). Gonca [64] first proposed this criterion for the Brayton power cycle. Moreover, commonly used power cycles such as reheated and inter-cooled Brayton cycles with variable specific heat [65–67], combined gas-steam [68], combined gas-mercury-steam [69], combined dual-Miller-Rankine [70], and diesel cycles [71] have also been analyzed and the effects of design parameters on performance criteria investigated. Generally, the results show that using EFECPOD during the design phase allows more realistic inferences.

Another criterion this study will examine is mean exergy density (or mean cycle pressure; MCP), which gives the net exergy output per unit volume change. Karakurt [72] proposed this criterion, which considers the relationship between dimension and performance together, and applications for diesel, Otto, and Atkinson power cycles [73] and Brayton power cycles [74] have been implemented within this scope. Studies have generally found the thermal efficiency value to be 1-2% higher and the net specific work to be around 10-12% higher under the conditions where the MCP value is at its maximum. However, smaller systems can be designed under the same conditions by optimizing the MCP value.

This study discusses the effects the oxygen density and pressure ratio have on exergy efficiency, power density (PD), EPC, ECOP, EFECPOD, MED, and COPD, which all evaluate performance, size, and economic outputs together, in oxy-combustion processes. Thus, the advantages and disadvantages of the oxy-combustion system compared to the conventional gas turbine power system are revealed.

The lack of comparative studies based on so many different criteria for oxy-fuel combustion processes in the literature has been the main motivation for this study. Thus, the shortcomings of environmentally friendly oxy-combustion power systems will be seen. It will be used as a guide for future studies.

## THEORETICAL MODEL AND SIMULATION

As seen in Figure 1, the conventional gas turbine power system and oxy-combustion power systems have common components (i.e., compressor, combustion chamber, turbine, and regenerator / regenerative heat exchanger). The only different component is a cooler used to separate water in the oxy-combustion power systems. While many different combinations are possible for oxy-combustion power cycles, the reason for this simplification is to clearly demonstrate the comparison through a thermodynamic analysis. Detailed thermodynamic analyses have been made based on the following assumptions:

- All gases are considered ideal; enthalpy and specific heats change with temperature.
- The fuel selected for analyses is natural gas in gaseous form, containing 92.03% CH<sub>4</sub>, 5.75% C<sub>2</sub>H<sub>6</sub>, 1.31% C<sub>3</sub>H<sub>8</sub>, 0.45% C<sub>4</sub>H<sub>10</sub>, 0.46% N<sub>2</sub>; combustion is adiabatic [75,76].
- The air supplied for combustion is completely dry and contains only 0.21 mol O<sub>2</sub> and 0.79 mol N<sub>2</sub>.
- For the unburned air/oxygen and fuel mixture, the reactant temperature is equal to the compressor outlet temperature and the fuel temperature is assumed to be equal to the ambient temperature.
- Combustion is assumed to occur at a steady state, the combustion chamber to be a well-stirred reactor (WSR), and the primary zone residence time to be 0.002 seconds.
- Compressor and turbine efficiency is 88%.
- The study's working fluid has a constant flow and a constant turbine inlet temperature.
- According to Lefebvre, the pressure loss in the combustion chamber varies between 2.5% and 5% [77]. Therefore, combined pressure loss in the combustion chamber due to friction, turbulence, and temperature rise including the pressure loss in the turbine is assumed to be 4% in total.

In order to find the optimum operating performance of the systems, a numerical simulation has been prepared using Matlab software. With this Matlab code, much faster and more accurate results have been obtained parametrically. The pressure, temperature, specific heat, enthalpy, and entropy values for each component in the plant have been calculated in order to compare the conventional gas turbine power plant with the oxy-combustion power plant. The energy equations of the energy systems shown in Figure 1 are as follows:

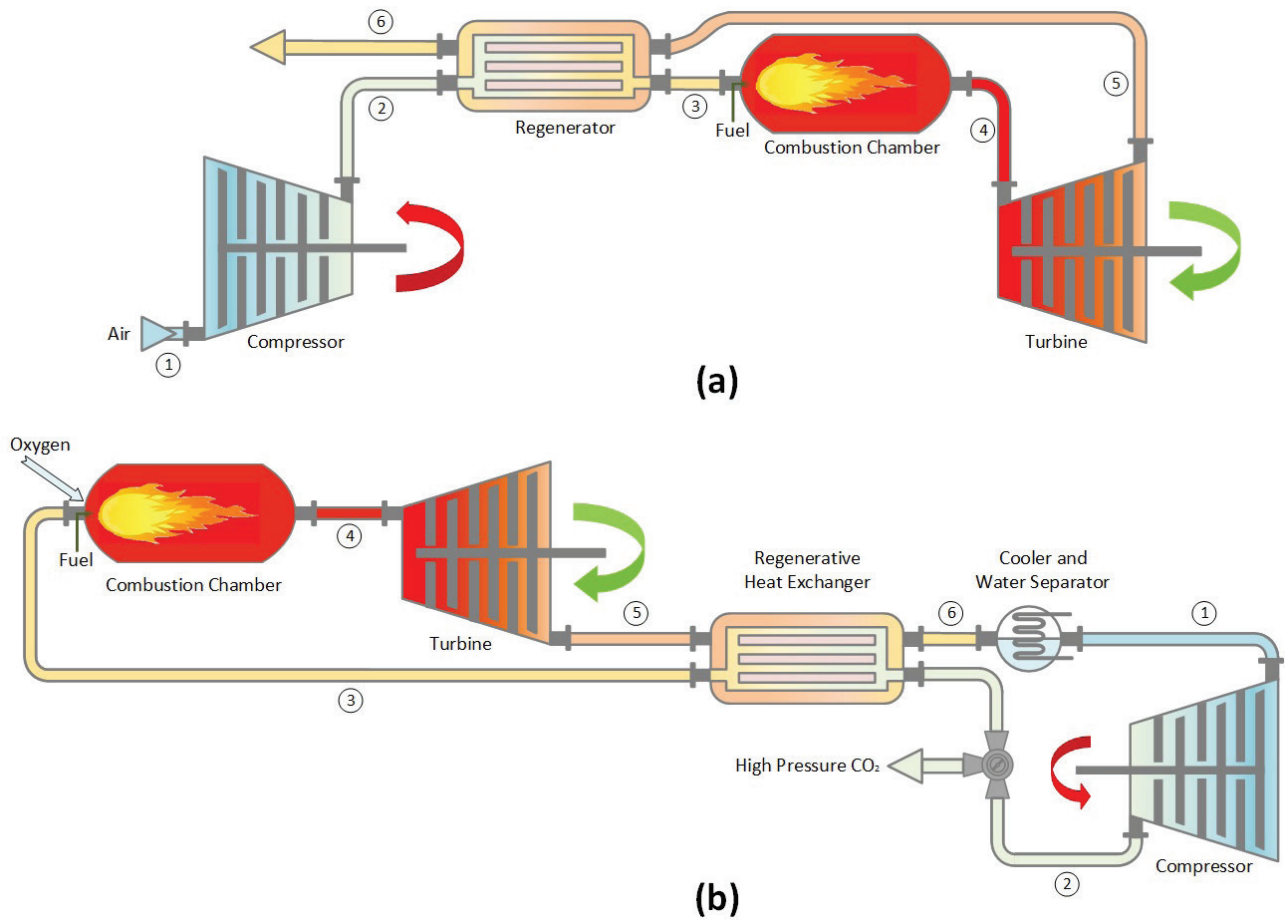


Figure 1. Conventional gas turbine power plant diagram (a) and oxy-fuel combustion power plant diagram (b).

**Compressor**

The compressor outlet temperatures vary according to the pressure ratio; the  $k$  value has been taken for air in the conventional gas turbine system and for  $CO_2$  in the oxy-combustion power system.

$$T_2 = T_1 \left( 1 + \frac{1}{\eta_c} \left( Pr^{\frac{k-1}{k}} - 1 \right) \right) \tag{1}$$

$$\dot{W}_C = \dot{m}_{ox} c_p (T_2 - T_1) \tag{2}$$

Calculating the compressor work, the  $c_p$  values are calculated for air and  $CO_2$ . The  $c_p$  values vary based on temperature.

$$c_{p,g}(T) = [a_1 + a_2 T + a_3 T^2 + a_4 T^3 + a_5 T^4] R_u \tag{3}$$

**Regenerator/Regenerative Heat Exchanger**

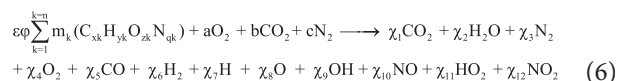
$$\dot{m}_{ox} (h_3 - h_2) = \dot{m}_T (h_5 - h_6) \eta_r \tag{4}$$

Regenerator pressure loss and efficiency are important for calculation.

$$P_3/P_2 = (1 - \Delta P_r) \tag{5}$$

**Combustion Chamber**

The turbine inlet temperature remains constant in all gas turbine power cycles. The reason for this is the turbine blades can withstand temperatures up to (1,400° C) [78]. Also, pressure loss is very important for cycle efficiency. According to Richards [79], preventing a 5%-loss in pressure is as effective as doubling the compression ratio. The total pressure loss in the combustion chamber is considered to be 4% regarding turbulence, friction, and pressure losses at the turbine inlet. A combustion model has been created for calculating the thermodynamic properties more precisely. The combustion products are calculated as a function of the equivalence ratio and temperature by taking into account the equilibrium constants. The global chemical equation for the combustion model is as follows:



Here,  $X_1$  to  $X_{12}$  represent the number of moles for each species, and  $x, y, z,$  and  $q$  represent the number of carbon, hydrogen, oxygen, and nitrogen atoms in the fuel, respectively. Here,  $\varphi$  is the overall equivalence ratio, and  $\varepsilon$  is the molar air-fuel ratio calculated from the stoichiometric combustion of fuel.

$$f = \frac{FA}{FA_s} \tag{7}$$

$$\varepsilon = \frac{4a}{4X+Y-2Z} \tag{8}$$

Ferguson's combustion equilibrium method has been used as the basis for finding the 12 unknown mole fractions [80]. Equations 6 and 9 are needed to solve the mole fractions for the combustion products. Six of these are provided by the chemical kinetic rates of products. Four more equations have been obtained from the atomic balance of the combustion model in calculating the equilibrium products. The results have been obtained numerically. The system of equations has been solved iteratively using Newton-Raphson and Gauss-Seidel methods. The achieved results and their validation using the programs GASEQ and NASA CEA are detailed in the authors' studies [81–83]. The molar specific heat, enthalpy, and entropy values for each types can be obtained from the following expressions using the curve-fitting coefficients ( $a_1 \dots a_n$ ) for the thermodynamic properties of carbon, hydrogen, oxygen, and nitrogen (CHON) systems [84]:

$$\frac{\bar{h}_k}{R_u T} = a_{1,k} + \frac{a_{2,k}}{2} T + \frac{a_{3,k}}{3} T^2 + \frac{a_{4,k}}{4} T^3 + \frac{a_{5,k}}{5} T^4 + \frac{a_{6,k}}{2} \tag{9}$$

$$\frac{\bar{c}_{p,k}}{R_u} = a_{1,k} + a_{2,k} T + a_{3,k} T^2 + a_{4,k} T^3 + a_{5,k} T^4 \tag{10}$$

$$\frac{\bar{s}_k^0}{R_u T} = a_{1,k} \ln T + a_{2,k} T + \frac{a_{3,k}}{2} T^2 + \frac{a_{4,k}}{3} T^3 + \frac{a_{5,k}}{4} T^4 + a_{7,k} \tag{11}$$

At constant pressure, temperature-based changes in the mole fractions of the mixture cause the enthalpy of the mixture to change due to separations. The final specific heat of the gas mixture also changes as defined below:

$$h = \frac{1}{M} \sum_{k=1}^{12} \alpha_k \bar{h}_k \text{ [kJ/kg]} \tag{12}$$

$$\bar{s} = \frac{R_u}{M} \left[ \sum_{k=1}^n \alpha_k (\bar{s}_k^0 - \ln \alpha_k) - \ln \left( \frac{P}{P_0} \right) \right] \tag{13}$$

$$\left( \frac{\partial h}{\partial T} \right)_P = c_{p_g} = \sum_{k=1}^{12} \frac{\alpha_k}{M} \frac{\partial \bar{h}_k}{\partial T} + \frac{\bar{h}_k}{M} \frac{\partial \alpha_k}{\partial T} - \frac{\alpha_k \bar{h}_k}{M^2} \frac{\partial M}{\partial T} \tag{14}$$

$$\left( \frac{\partial h}{\partial T} \right)_P = c_{p_g} = \frac{1}{M} \left[ \sum_{k=1}^{12} \alpha_k \bar{c}_{p_k} + \bar{h}_k \frac{\partial \alpha_k}{\partial T} - h M_T \right] \tag{15}$$

$$M_T = \frac{\partial M}{\partial T} = \sum_{k=1}^{12} M_k \frac{\partial \alpha_k}{\partial T} \tag{16}$$

Here, the combustion temperature is  $T$  (in Kelvin). The product molar mass is  $M_k$ , and the total products molar mass is  $M$ .

$$M = \sum_{k=1}^{12} m_k = \sum_{k=1}^{12} \alpha_k M_k \tag{17}$$

The total number of moles in the products can be found by dividing the molecular weight of the combustion products by the mass of the reactants as follows, resulting in the number of moles  $y_1, y_2, y_3, \dots, y_{12}$  being obtained.

$$N = \frac{m_R}{M} \Rightarrow v_k = y_k N \tag{18}$$

To calculate the combustion chamber outlet temperature:

$$T_e = \frac{T_{pz} c_p m_{ox} + T_{cox} c_{p,cox} m_{cox}}{c_p m_{ox} + c_{p,cox} m_{cox}} \tag{19}$$

Here,  $T_{pz}$  is the primary zone air temperature, and  $T_{cox}$  is the dilution air temperature. In addition, the amount of heat generated in the combustion chamber is calculated using the following equation:

$$Q_{in} = \dot{m}_f LHV / \eta_{cc} \tag{20}$$

**Turbine**

$$T_5 = T_4 \left( 1 - \eta_T \left[ 1 - \left( \frac{P_4}{P_5} \right)^{\frac{1-k_g}{k_g}} \right] \right) \tag{21}$$

After obtaining the turbine outlet temperature,  $C_{p,g}$  is obtained from detailed calculation of the gas mixtures entering the turbine after combustion as in Equation 3.

$$\dot{W}_T = \dot{m}_T c_{p,g} (T_4 - T_5) \quad (22)$$

$$c_{p,g}(T) = [a_1 + a_2 T + a_3 T^2 + a_4 T^3 + a_5 T^4] R_u \quad (23)$$

Net power is found by subtracting the power generated in the turbine from the power consumed in the compressor:

$$\dot{W}_{NET} = \dot{W}_T - \dot{W}_C \quad (23)$$

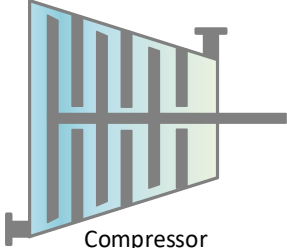
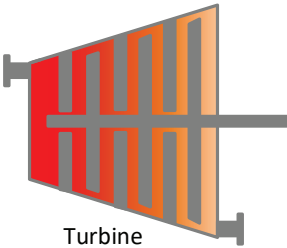
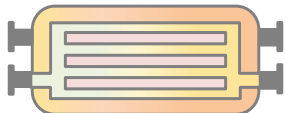
System efficiency is calculated from the following equation:

$$\eta = \dot{W}_{net} / \dot{Q}_{in} \quad (24)$$

Exergy is obtained with the physical exergy, chemical exergy, kinetic exergy and potential exergy. Kinetic exergy and potential exergy are assumed to be negligible. Physical exergy is defined as the maximum theoretical useful work obtained as a system interacts with an equilibrium state. The chemical exergy is associated with the system's chemical composition departing from its chemical equilibrium. Chemical exergy is an important part of exergy in combustion processes. The exergy equation can be written as follows:

$$\dot{E}X_Q + \sum_i \dot{E}X_i = \sum_o \dot{E}X_o + \dot{E}X_w + \dot{E}X_D \quad (25)$$

**Table 1.** Exergy destruction and exergy efficiency functions of system components

Components	Exergy Destruction	Exergy Efficiency
 <p>Compressor</p>	$E\dot{X}_{D,com} = \dot{W}_{com} + \dot{E}_i - \dot{E}_o$	$\eta_{ex,com} = \frac{\dot{E}_o - \dot{E}_i}{\dot{W}_{com}}$
 <p>Combustion Chamber</p>	$E\dot{X}_{D,cc} = \dot{E}_i + \dot{E}_{f,cc} - \dot{E}_o$	$\eta_{ex,cc} = \frac{\dot{E}_o}{\dot{E}_i + \dot{E}_{f,cc}}$
 <p>Turbine</p>	$E\dot{X}_{D,tur} = \dot{E}_i - \dot{E}_o - \dot{W}_{tur}$	$\eta_{ex,tur} = \frac{\dot{W}_{tur}}{\dot{E}_i - \dot{E}_o}$
 <p>Heat Exchanger/ Regenerator</p>	$E\dot{X}_{D,r} = \dot{E}_{i,1} + \dot{E}_{i,2} - \dot{E}_{o,1} - \dot{E}_{o,2}$	$\eta_{ex,r} = \frac{\dot{E}_{i,1} - \dot{E}_{o,1}}{\dot{E}_{i,2} - \dot{E}_{o,2}}$
 <p>Cooler and Water Separator</p>	$E\dot{X}_{D,cool} = \dot{E}_i - \dot{E}_o - \dot{E}_{out}$	$\eta_{ex,cool} = \left( 1 - \frac{\dot{E}_{out}}{\dot{E}_i - \dot{E}_o} \right)$

$$\dot{EX}_Q = \left(1 - \frac{T_0}{T_i}\right) \dot{Q}_i \tag{26}$$

$$\dot{EX}_W = \dot{W} \tag{27}$$

$$ex = ex_{ph} + ex_{ch} \tag{28}$$

$$ex_{ph} = (h_k - h_0) - T_0 (s_k - s_0) \tag{29}$$

$$ex_{ch} = x_k ex_{Ch}^k + RT_0 \sum x_k \ln x_k \tag{30}$$

One of the most important performance criteria for power systems is power density, definable as the ratio of produced power to the maximum volume of the system. It was first proposed by Sahin et. al. [13] for an endoreversible Carnot heat engine. Maximizing the power density gives an approach to the most appropriate engine with respect to power per volume and supports less weight and more volume. In this context, the effective power density (*PD*) is found as follows:

$$P_D = \frac{P_{ef}}{V_T} \tag{31}$$

where  $P_{ef}$  and  $V_T$  are effective power and maximum volume of the system, respectively.

As a beneficial output of the second law of thermodynamic for all kinds of thermal systems, exergy efficiency is defined in Eq.32 as the ratio of effective power to fuel exergy for the analyzed system,

$$\eta_{ex} = \frac{P_{ef}}{\dot{m}_f \psi_f} \tag{32}$$

where  $P_{ef}$ ,  $\dot{m}_f$  and  $\psi_f$  are effective power, fuel flow rate, and total exergy of fuel.

The exergetic performance coefficient (EPC) was proposed by Ust et al. [27] as the ratio of total exergy output to the exergy destruction rate in a cogeneration system (see Equation 33). EPC defines how a system or component destroys exergy efficiently with respect to the total irreversibilities or total exergy destruction,

$$EPC = \frac{EX_{out}}{T_0 S_i} = \frac{EX_{out}}{EX_{D,tot}} = \frac{EX_{in}}{EX_{D,tot}} - 1 \tag{33}$$

where  $T_0$  and  $S_i$  refer to ambient temperature and total entropy generation; the *EX* subscripts of *out*, *in*, and *D*, *tot*

refer to exergy output, exergy inlet, and exergy destruction, respectively.

Another important exergetic performance criterion for thermal systems is the ecological coefficient of performance criterion (ECOP), also first suggested by Ust et al. [43] for an irreversible Seilinger (i.e., dual) cycle. It is defined in Equation 34 as the ratio of effective power to the total exergy destruction rate; this also makes a realistic combination of the first and second laws of thermodynamics.

$$ECOP = \frac{P_{ef}}{EX_D} \tag{34}$$

Another current thermoecological performance criterion is effective ecological power density (EFECPOD), which provides invaluable connections using a realistic finite time model among the effective efficiency, effective power, cycle temperature ratio, and volume. The criterion first suggested by Gonca [64] for a gas turbine is defined as:

$$EFECPOD = \frac{\eta_{ef} P_{ef}}{\frac{T_1}{T_0} \alpha V_T} \tag{35}$$

where  $\eta_{ef}$  and  $P_{ef}$  refer to effective efficiency and effective power,  $T_1$  and  $T_0$  refer to the temperature of air intake for the compression cycle and ambient conditions,  $V_T$  refers to total volume, and  $\alpha$  refers to the ratio of the cycle's maximum:minimum temperature.

The cycle's mean cycle pressure (MCP) or mean exergy density (MED) is another important definition for thermal systems that makes a beneficial comparison of performance with the dimensions/size of the system. It was proposed by Karakurt and Sahin [73] for a Brayton cycle as the ratio of net exergy production to the volumetric change (see Eq. 36). It is equal to the mean effective pressure if the compression and expansion processes are ideal or isentropic efficiencies are 1:

$$MED = \frac{P_{ef}}{v_{max} - v_{min}} \tag{36}$$

where  $P_{ef}$ ,  $v_{max}$  and  $v_{min}$  refer to the cycle's net exergy production, maximum volume, and minimum volume. Examining all these thermodynamic criteria in detail allows for viewing the results that will be shown in many graphs the parameters created on useful work and power density. This also presents the results clearly with a single output when examining power systems under different conditions and states. As a result of detailed research on this subject, thermodynamic coefficients have been revealed in ecological terms while no economic study is observed. For this reason, intensive research has been made on a parameter that will directly provide effective results when comparing the

results of the analysis in this area, which reveals the power density cost coefficient:

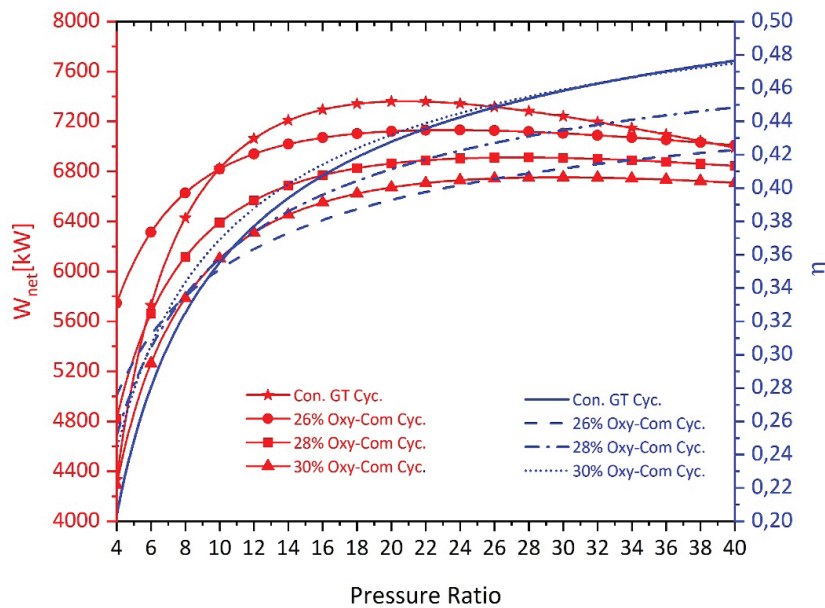
$$COPD = \frac{E \frac{T_{max}}{T_{min}} V_T}{P_{ef} \eta_{ef}} \left[ \frac{\$}{kJ \times m^3} \right] \quad (37)$$

**RESULTS AND DISCUSSION**

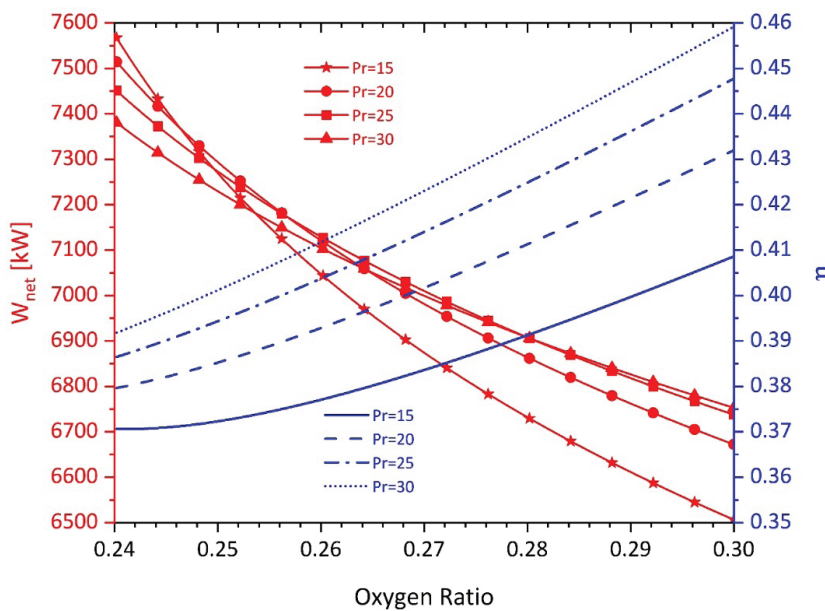
The results from the exergetic analyses of the conventional gas turbine power system and oxy-combustion power

systems are presented in Figures 2 through 6. Net power, efficiency, exergy destruction, exergy efficiency, power density, EPC, ECOP, EFECPOD, MED, and COPD have been calculated with respect to various pressure and oxygen ratios, the results of which are shown in these figures.

Figures 2a and 2b show the effects changes in pressure and oxygen ratios have on system net power and efficiency. As seen in Figure 2a, the net power generated from the system increases rapidly up to 20.8 (PR) in conventional gas turbine power systems. A slight decrease occurs after the peak point of maximum net power. These results are similar for the oxy-combustion power systems. In the oxy-combustion



(a)

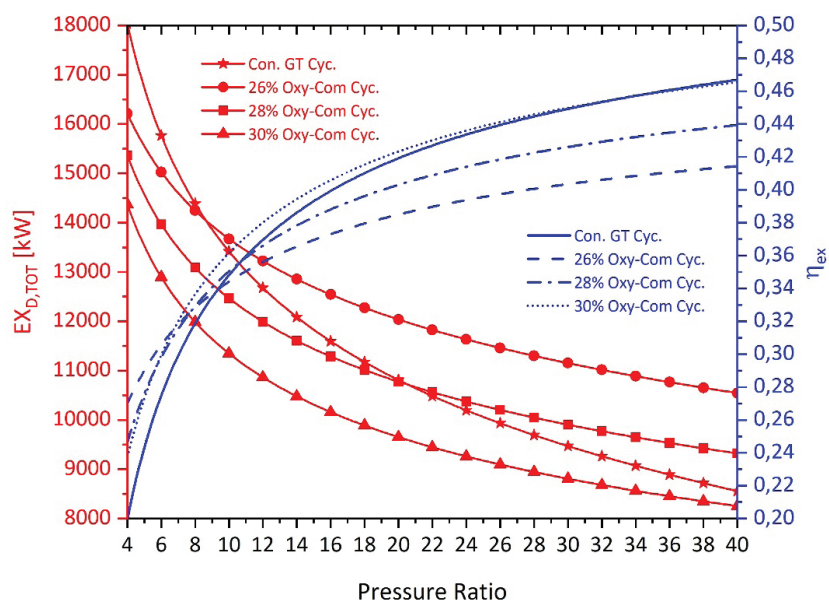


(b)

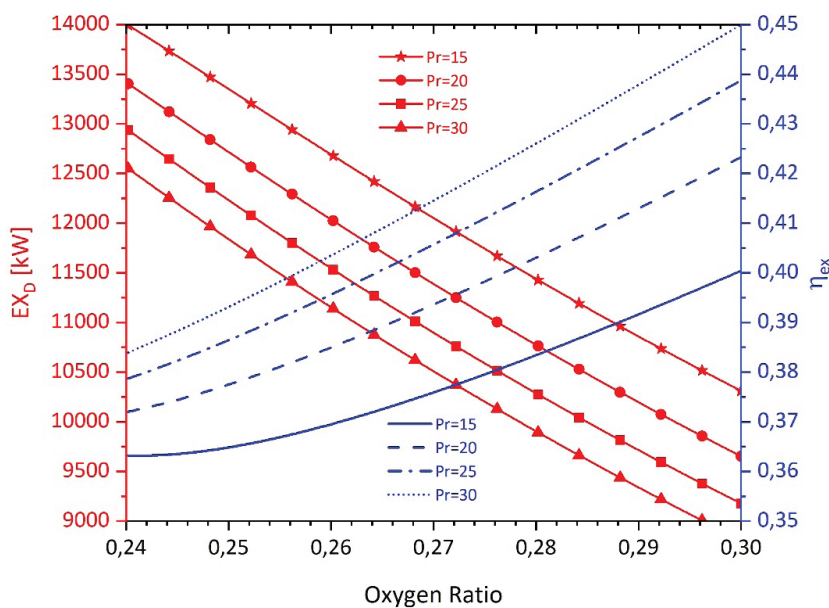
**Figure 2.** (a) Change in net power and efficiency in terms of pressure ratios for various oxygen rates; (b) Change in net power and efficiency in terms of oxygen ratios for various pressure ratios.

power systems, the decrease after the peak point is less than that in conventional gas turbine power systems. The maximum net powers obtained for the peak points in the oxy-combustion power systems are 23.3, 27.4, and 29.7 in the 26%, 28%, and 30% oxy-combustion power systems, respectively. In terms of the net power produced, better results are seen to have been obtained in the conventional gas turbine power system compared to the oxy-combustion power systems for pressure ratios above 10. For pressure ratios between 4 and 10, the 26% oxy-combustion power system is seen to produce more net power. Additionally, the

conventional gas turbine power system shows better results in terms of heat added to the system compared to the 26% oxy-combustion power system for pressure ratios up to 8. Similarly, the overall efficiency of the system increases and specific fuel consumption decreases with increases in the pressure ratio. Conventional gas turbine power systems are better than the 28% oxy-combustion power cycle at pressure ratios up to 8. The reason for this is that, although the net power obtained from conventional gas turbine power systems is high, the heat added to the system is also high. The 30% oxy-combustion power cycle up to pressure ratios



(a)



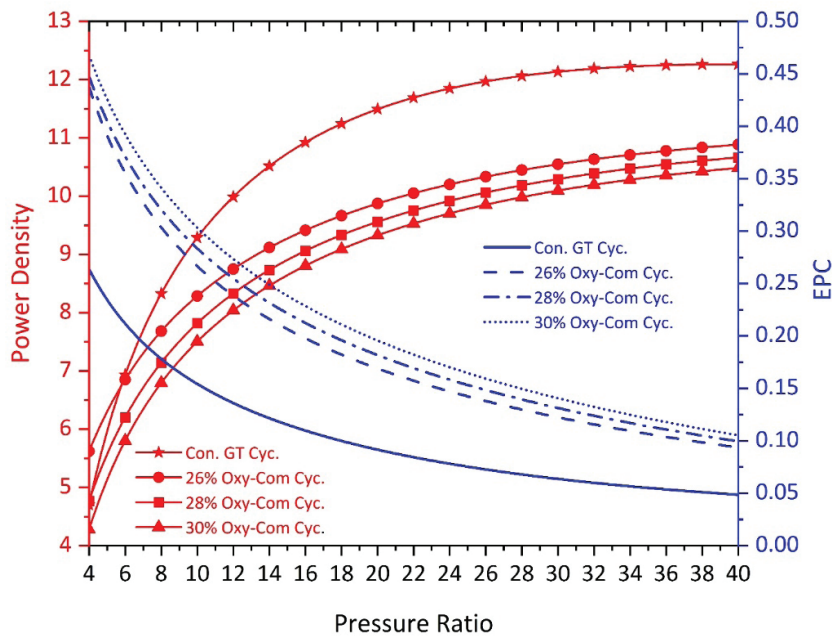
(b)

**Figure 3.** (a) Change in exergy destruction and exergy efficiency with respect to pressure ratios for various oxygen fractions, (b) Change in exergy destruction and exergy efficiency with respect to oxygen ratios for various pressure ratios.

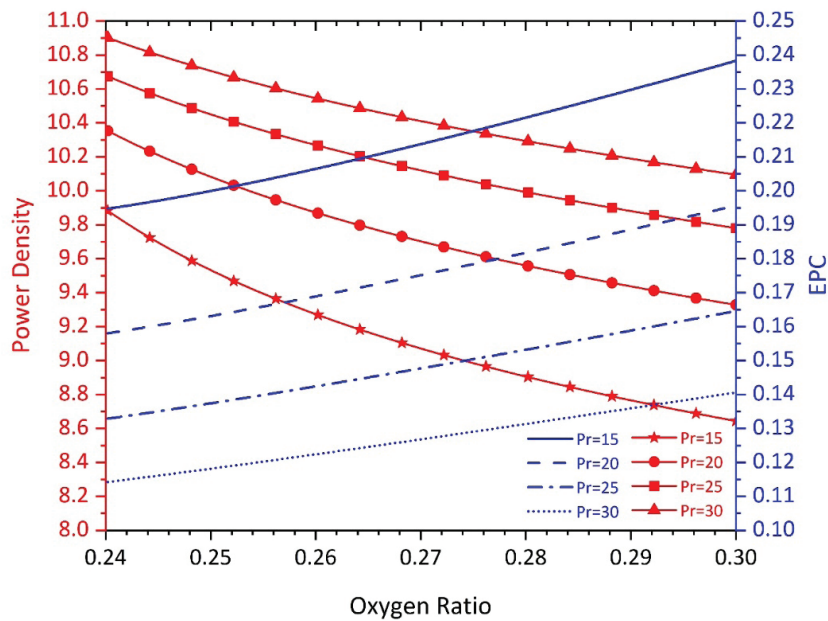
of 35.3 has the best performance in terms of efficiency. As can be seen in Figure 2b, the net power obtained by increasing the oxygen ratio in oxy-combustion power systems has been determined to decrease. In addition, as the pressure ratio increases from 15 to 30, these decreases are seen to lessen. However, the oxy-combustion power cycle's efficiency increases as oxygen and pressure ratios increase.

Figures 3a and 3b show the effect variations in pressure and oxygen rates have on the total exergy destruction and exergy efficiency of the systems. As seen in Figure 3a,

the total exergy destruction in the system decreases as the pressure ratio increases in both the oxy-combustion power cycles and conventional gas turbine power system. This downward trend appears to be greater in the conventional gas turbine power system compared to the oxy-combustion power systems. In the conventional gas turbine power system, total exergy destruction is greater than all oxy-combustion gas turbine power cycles up to the 8.6 pressure ratio. It also has more exergy destruction compared to the oxy-combustion power cycles with a 28% oxygen ratio up



(a)

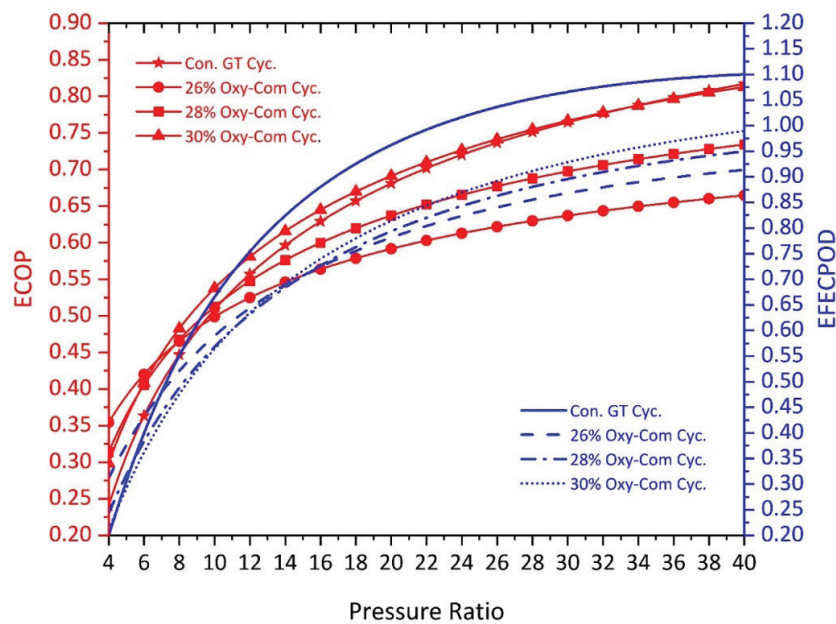


(b)

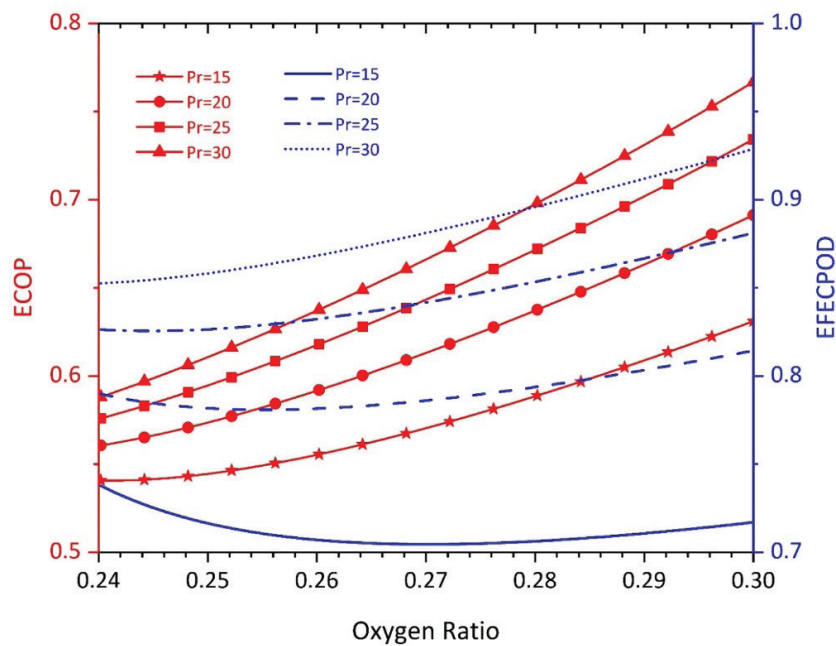
**Figure 4.** (a) Change in power density and EPC with respect to pressure ratio for various oxygen rates, (b) Change in power density and EPC with respect to oxygen ratio for various pressure ratios.

to a pressure ratio of 20.6. The best results regarding total exergy destructions are obtained for the oxy-combustion power cycle at the 30% oxygen ratio. When examined in terms of exergy efficiency, all cycles increase less and less as the pressure ratio increases. Oxy-combustion power cycles with a pressure ratio of up to 10 have higher exergy efficiency than the conventional gas turbine power cycle. In the oxy-combustion power systems, oxygen ratio increasingly have the highest exergy efficiency from 26% to 30%

up to a pressure ratio of 33.2, above which the conventional gas turbine power systems have the highest exergy efficiency. As seen in Figure 3b, the total exergy destruction decreases with increases in both the oxygen and pressure ratios. Meanwhile, as these two effects increase, so does the exergy efficiency. These results are seen to converge as the the pressure ratio increases from 15 to 30. Namely, the pressure ratio differences between 25 and 30 are less than the differences between 15 and 20.



(a)

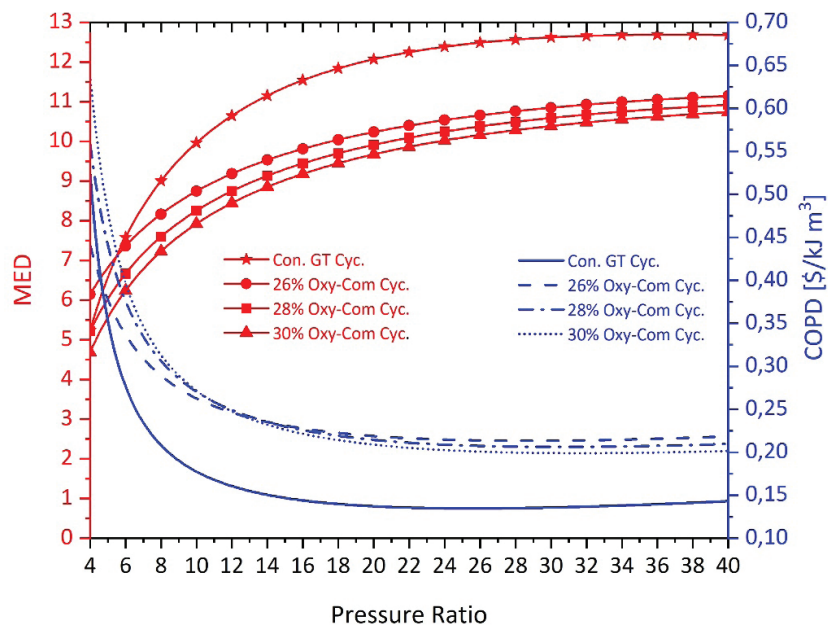


(b)

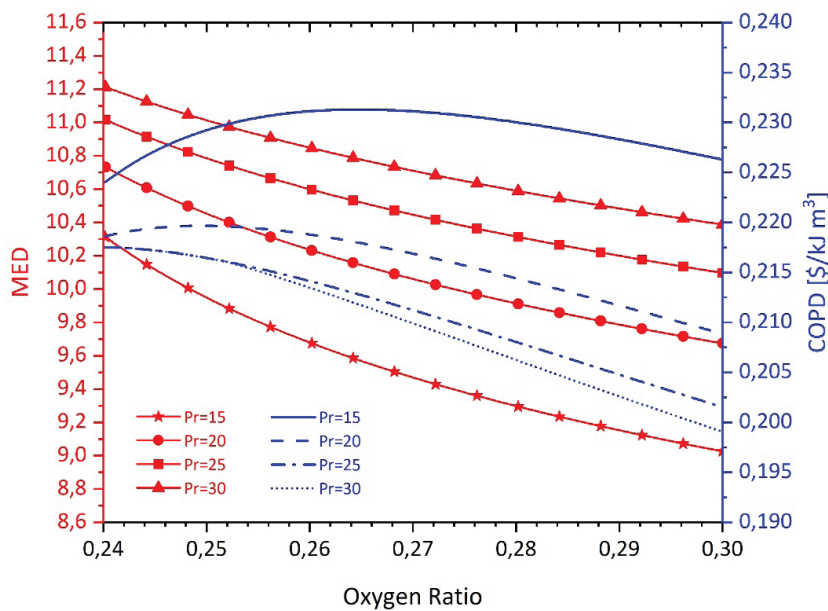
**Figure 5.** Changes in ECOP and EFECPOD with respect to pressure ratio for various oxygen rates, (b) Changes in heat added and net power with respect to oxygen rates for various pressure ratios.

Figures 4a and 4b show the effect variations in pressure and oxygen rates have on the systems' power density and exergetic performance coefficients. As seen in Figure 4a, the conventional gas turbine power cycle has better results showing slightly higher power density compared to the oxy-combustion power cycles in terms of power density. In addition, the cooling and water separation unit allows the oxy-combustion power systems to give off zero harmful emissions; the oxygen is provided by a separate mechanism, and the valve equipment used to separate excess carbon

dioxide from the total volume is high. The oxy-combustion power cycles with 26%, 28% and 30% oxygen rates have similar characteristics in terms of power density, with the power density observed to decrease slightly as oxygen rates increase. When examined in terms of the exergetic performance coefficient, the amount of exergy output is observed to be less in the conventional gas turbine power cycle compared to the oxy-combustion power systems. As seen in Figure 4b, increasing the oxygen rates in oxy-combustion power systems decrease the power density, while increasing



(a)



(b)

**Figure 6.** (a) Changes in exergy density and COPD with respect to pressure ratio for various oxygen rates, (b) Changes in exergy density and COPD with respect to oxygen rates for various pressure ratios.

the pressure ratio increases the power density. The opposite occurs when examined in terms of the exergetic performance coefficient. In the oxy-combustion power cycle systems, increases in oxygen rates increase the exergetic performance coefficient, while increases in the pressure ratio decrease the exergetic performance coefficient.

Figures 5a and 5b show the effect variations in pressure ratios and oxygen rates have on the systems' ecological performance coefficient and effective ecological power density. As can be seen in Figure 5a, the ecological performance coefficient increases both in the conventional gas turbine power system and in the oxy-combustion power systems less and less with greater increases in the pressure ratio. Above pressure ratios of 20, the ecological performance coefficient in the conventional gas turbine and the 30% oxy-combustion power systems are practically the same. While the 28% oxy-combustion power system has a slightly lower value compared to the conventional gas turbine system, the lowest ecological performance coefficient results are achieved in the 26% oxy-combustion power system. When analyzing the effective ecological power density, the conventional gas turbine power system is seen to have a slightly higher value than the oxy-combustion power systems. The effective ecological power densities in the oxy-combustion power systems intersect at the pressure ratio of 14.5. Below this pressure, the order of the effective ecological power density results according to the oxygen ratio differ; above this pressure, the effective ecological power density increases as oxygen rates increase from 26% to 30%. As seen in Figure 5b, the ecological performance coefficient increases as both the oxygen rates and pressure ratios increase in the oxy-combustion power systems. Meanwhile, when examining the effective ecological power density, increases in the pressure ratio directly and proportionally affect EFECPOD, continuing to increase as the oxygen ratio increases after a certain decrease, due to the efficiency and power factors in the effective ecological power density increasing differently for oxy-combustion power cycles with different oxygen rates. In other words, increases in oxygen rates may cause efficiency to increase or decrease in terms of net power obtained.

Figures 6a and 6b show the effect variations in pressure and oxygen rates have on systems' exergy density and cost of power density. As seen in Figure 6a, the conventional gas turbine power cycle has better results than the oxy-combustion power cycles in terms of exergy density. The oxy-combustion power cycles with 26%, 28% and 30% oxygen ratios have similar characteristics in terms of exergy density, with the exergy density observed to decrease slightly as the oxygen rates increase. Examining the power density in terms of cost, the conventional gas turbine power cycle can be seen to cost less than the oxy-combustion power systems because, as mentioned earlier, the oxy-combustion power systems take up slightly more space and are slightly more costly. In other words, economically comparing power systems can be achieved with just one graph. When evaluating using the realized economic results, how quickly the cost of power

density parameter can be seen allows clearer and more accurate results to be obtained. As can be seen in Figure 6, increases in the oxygen rates in oxy-combustion power systems decrease the exergy density, while increases in the pressure ratio increase the exergy density. When examining the power density in terms of cost, a different characteristic emerges. Higher oxygen rates in the oxy-combustion power cycle systems decrease the cost of power density after increasing by a certain amount at pressure ratios of 15 and 20, while increases at the 25 and 30 pressure ratios directly decrease these costs.

## CONCLUSION

This study has performed detailed exergetic analyses of the conventional gas turbine power cycle and environmentally promising oxy-combustion power cycle systems. Parametric analyses results have been obtained for pressure ratios from 4 to 40 and oxygen rates ranging from 24% to 30%. The net power increases rapidly in both the conventional gas turbine power cycle and the oxy-combustion power cycles with increases in the pressure ratio, continuing to increase less and less after reaching its peak. The maximum net power point in the conventional gas turbine power cycle is 20.8. The peak points in the oxy-combustion power cycles with 26%, 28%, and 30% oxygen rates are 23.3, 27.4, and 29.7, respectively. The net power obtained by increasing the oxygen ratio decreased. System efficiencies increase as both the pressure ratio and oxygen rates increase; as the incoming heat decreases, the net power. As the pressure ratio increases, the total exergy destruction in both conventional gas turbine power system and oxy-combustion power systems decreases. In oxy-combustion power systems, increases in the oxygen rate decrease the total exergy ratio. However, increases in the pressure ratio and the oxygen rate increase the exergy efficiency. In terms of power density, higher results have been obtained in the conventional gas turbine power system compared to the oxy-combustion power systems. Increasing the pressure ratio increases the power density in all systems. In oxy-combustion power systems, increases in oxygen rates decrease the power density. The opposite result is achieved for the exergetic performance coefficient. Increases in the pressure ratio and/or oxygen rate increase the ecological performance coefficient. Likewise, while increases in the pressure ratio cause increases in the effective ecological power density, increases in the oxygen rate in the oxy-combustion power systems show different characteristics according to the cycle's pressure ratio. In terms of cost of power density, the conventional gas turbine power system is more advantageous than oxy-combustion power systems. The optimum cost of power density is obtained at the pressure ratio of 25.6. Oxy-combustion power systems have a minimum power density at 26%, 28%, and 30% oxygen rates with respective values of 28.6, 30.5, and 31.65. Increases in the oxygen rate in the oxy-combustion power cycle decrease

the cost of power density after specific increases at pressure ratios of 15 and 20, while increases at pressure ratios of 25 and 30 directly decrease the cost of power density. Oxy-combustion power cycles currently have higher costs compared to conventional gas turbine power cycles. However, oxy-combustion power cycles will become more popular due to the decreasing cost of pure oxygen with technological developments and increasing environmental sensitivities in the following years.

## NOMENCLATURE

a	mole number of reactant O <sub>2</sub>
b	mole number of reactant CO <sub>2</sub>
c	mole number of reactant N <sub>2</sub>
C	specific heat (kJ/kg K)
FA	fuel/air ratio
h	specific enthalpy (kJ/kg)
LHV	lower heat value
N	total number of moles of species
NG	natural gas
Pr	pressure ratio
s	specific entropy (kJ/kg K)
SFC	specific fuel consumption
T	temperature (K)
X	total number of carbon atom
Y	total number of hydrogen atoms
Z	total number of oxygen atoms
Q	total number of nitrogen atoms
Q	heat

### Greek symbols

$\alpha$	mole fraction / Temperature ratio
$\epsilon$	molar air-fuel ratio $\eta_{ex}$
$\Phi$	equivalence ratio
$\chi$	number of moles of exhaust species
$\psi$	Fuel exergy

### Subscripts

a	air
ady	adiabatic
c	compressor
cc	combustion chamber
fu	fluid or oxidant
in	inlet
k	exhaust species
pz	primary zone
r	reactants
ox	oxidant
oxy	oxygen
wf	working fluid
t	turbine
x	number of carbon atoms
y	number of hydrogen atoms
z	number of oxygen atoms
q	number of nitrogen atoms

## AUTHORSHIP CONTRIBUTIONS

Authors equally contributed to this work.

## DATA AVAILABILITY STATEMENT

The authors confirm that the data that supports the findings of this study are available within the article. Raw data that support the finding of this study are available from the corresponding author, upon reasonable request.

## CONFLICT OF INTEREST

The author declared no potential conflicts of interest with respect to the research, authorship, and/or publication of this article.

## ETHICS

There are no ethical issues with the publication of this manuscript.

## REFERENCES

- [1] İlhami Y, MacEachern C. 1.2 Historical aspects of energy. In: Dincer I, editor. Comprehensive energy systems. 1st ed. Oxford: Elsevier; 2018. pp. 24–48. [CrossRef]
- [2] International Energy Agency. Global Energy Review: CO<sub>2</sub> Emissions in 2020 - Analysis and findings. Paris: International Energy Agency; 2021.
- [3] Dincer I, Acar C. A review on clean energy solutions for better sustainability. Int J Energy Res 2015;39:585–606. [CrossRef]
- [4] Celiktas B. Experimental studies on cooling/compressing of carbon dioxide captured from oxy combustion. Master's Thesis. Istanbul, Turkey: Istanbul Technical University; 2016.
- [5] Allison T. Oxy-Fuel Combustion. Southwest Res Inst 2019. Available at: <https://www.swri.org/industry/advanced-power-systems-conventional-power-generation/oxy-fuel-combustion> Accessed on May 16, 2021.
- [6] Cannone SF, Lanzini A, Santarelli M. A Review on CO<sub>2</sub> capture technologies with focus on CO<sub>2</sub>-enhanced methane recovery from hydrates. Energies 2021;14:387. [CrossRef]
- [7] Zincir BA. Comparison of the carbon capture systems for onboard application and voyage performance investigation by a case study. Master's Thesis. Istanbul, Turkey: Istanbul Technical University; 2020.
- [8] LexInnova. Oxy-fuel Combustion Systems (OCS). Gurgaon: LexInnova; 2013.
- [9] Jurado N, Darabkhani HG, Anthony EJ, Oakey JE. Oxy-fuel combustion for carbon capture and sequestration (CCS) from a coal/biomass power plant: experimental and simulation studies. In: Dincer I, Colpan CO, Kizilkan O, Ezan MA, editors. Progress in Clean Energy Novel Systems and Applications. 1st ed. Berlin: Springer International Publishing; 2015. pp. 177–192. [CrossRef]

- [10] Gunduz Raheem D. Modeling of oxygen-enriched and oxy-combustion of lignite in cfbc and verification with experiments. Doctoral Thesis. Istanbul, Turkey: Marmara University; 2020.
- [11] Canada Natural Resources. Near-zero emissions oxy-fuel combustion. <https://www.nrcan.gc.ca/2016>. Available at: <https://www.nrcan.gc.ca/our-natural-resources/energy-sources-distribution/clean-fossil-fuels/coal-co2-capture-storage/carbon-capture-storage/near-zero-emissions-oxy-fuel-combustion/4307> Accessed on April 28, 2021.
- [12] Napp T, Sum KS, Hills T, Fennell PS. Attitudes and Barriers to Deployment of CCS from Industrial Sources in the UK. London: Imperial College; 2014.
- [13] Sahin B, Kodal A, Yavuz H. Efficiency of a Joule-Brayton engine at maximum power density. *J Phys Appl Phys* 1995;28:1309. [CrossRef]
- [14] Şahin B, Kodal A, Yavuz H. Maximum power density for an endoreversible carnot heat engine. *Energy* 1996;21:1219–1225. [CrossRef]
- [15] Kodal A. Maximum power density analysis for irreversible combined Carnot cycles. *J Phys Appl Phys* 1999;32:2958. [CrossRef]
- [16] Maheshwari G, Khandwawala DAI, Kaushik DSC. Maximum power density analyses for an irreversible radiative heat engine. *Int J Ambient Energy* 2005;26:71–80. [CrossRef]
- [17] Chen L, Zheng J, Sun F, Wu C. Performance comparison of an irreversible closed Brayton cycle under maximum power density and maximum power conditions. *Exergy Int J* 2002;2:345–351. [CrossRef]
- [18] Chen L, Zheng J, Sun F, Wu C. Performance comparison of an endoreversible closed variable temperature heat reservoir Brayton cycle under maximum power density and maximum power conditions. *Energy Convers Manag* 2002;43:33–43. [CrossRef]
- [19] Sahin B, Kodal A, Kaya SS. A comparative performance analysis of irreversible regenerative reheating Joule-Brayton engines under maximum power density and maximum power conditions. *J Phys Appl Phys* 1998;31:2125. [CrossRef]
- [20] Chen L, Wang J, Sun F. Power density analysis and optimization of an irreversible closed intercooled regenerated Brayton cycle. *Math Comput Model* 2008;48:527–540. [CrossRef]
- [21] Wang J, Chen L, Sun F. Power Density optimization of an irreversible closed intercooled regenerated brayton cycle coupled to variable-temperature heat reservoirs. In: Cen PK, Chi PY, Wang DF, editors. *Challenges of Power Engineering and Environment Proceedings of the International Conference on Power Engineering*; 2007 Apr 12-14; Setubal, Portugal: IEEE; 2007. pp. 928–934. [CrossRef]
- [22] Sahin B, Kesgin U, Kodal A, Vardar N. Performance optimization of a new combined power cycle based on power density analysis of the dual cycle. *Energy Convers Manag* 2002;43:2019–2031. [CrossRef]
- [23] Atmaca M, Gumus M, Demir A. Comparative thermodynamic analysis of dual cycle under alternative conditions. *Therm Sci* 2011;15:953–960. [CrossRef]
- [24] Al-Sarkhi BA, Abu-Nada IAH. Efficiency of atkinson engine at maximum power density using temperature dependent specific heats. *Jordan J Mech Ind Eng* 2008;2:71–75.
- [25] Ust Y. A Comparative performance analysis and optimization of the irreversible atkinson cycle under maximum power density and maximum power conditions. *Int J Thermophys* 2009;30:1001–1013. [CrossRef]
- [26] Atmaca M, Gumus M. Power and efficiency analysis of diesel cycle under alternative criteria. *Arab J Sci Eng* 2014;39:2263–2270. [CrossRef]
- [27] Ust Y, Sahin B, Yilmaz T. Optimization of a regenerative gas-turbine cogeneration system based on a new exergetic performance criterion: Exergetic performance coefficient. *Proc Inst Mech Eng Part J Power Energy* 2007;221:447–456. [CrossRef]
- [28] Ust Y, Sahin B, Kodal A. Optimization of a dual cycle cogeneration system based on a new exergetic performance criterion. *Appl Energy* 2007;84:1079–1091. [CrossRef]
- [29] Ust Y, Arslan F, Ozsari I, Cakir M. Thermodynamic performance analysis and optimization of DMC (Dual Miller Cycle) cogeneration system by considering exergetic performance coefficient and total exergy output criteria. *Energy* 2015;90:552–559. [CrossRef]
- [30] Ust Y, Akkaya AV, Safa A. Analysis of a vapour compression refrigeration system via exergetic performance coefficient criterion. *J Energy Inst* 2011;84:66–72. [CrossRef]
- [31] Ust Y, Karakurt AS. Analysis of a cascade refrigeration system (CRS) by using different refrigerant couples based on the exergetic performance coefficient (EPC) criterion. *Arab J Sci Eng* 2014;39:8147–8156. [CrossRef]
- [32] Ust Y, Karakurt AS, Gunes U. Performance analysis of multipurpose refrigeration system (MRS) on fishing vessel. *Pol Marit Res* 2016;23:48–56. [CrossRef]
- [33] Karakurt AS, Ozsari I, Bashan V. Exergetic performance analysis of high pressure air systems on ships. *Int J Exergy* 2022;37:74. [CrossRef]
- [34] Ust Y. Enerji üretim sistemlerinin ekolojik performans analizi ve optimizasyonu. PhD Thesis. Istanbul, Turkey: Yıldız Teknik University; 2005.
- [35] Ust Y, Arslan F, Ozsari I, Cakir M. Thermodynamic performance analysis and optimization of DMC (Dual Miller Cycle) cogeneration system by considering exergetic performance coefficient and total exergy output criteria. *Energy* 2015;90:552–559. [CrossRef]
- [36] Ust Y, Arslan F, Ozsari I. A comparative thermo-ecological performance analysis of generalized irreversible solar-driven heat engines. *Renew Energy* 2017;113:1242–1249. [CrossRef]

- [37] Angulo-Brown F. An ecological optimization criterion for finite time heat engines. *J Appl Phys* 1991;69:7465–7469. [\[CrossRef\]](#)
- [38] Ust Y. Ecological performance analysis of irreversible OTTO cycle. *J Eng Nat Sci* 2005;29:106–117.
- [39] Ust Y, Sahin B, Kodal A. Ecological coefficient of performance (ECOP) optimization for generalized irreversible Carnot heat engines. *J Energy Inst* 2005;78:145–151. [\[CrossRef\]](#)
- [40] Wu H, Ge Y, Chen L, Feng H. Power, efficiency, ecological function and ecological coefficient of performance optimizations of irreversible Diesel cycle based on finite piston speed. *Energy* 2021;216:119235. [\[CrossRef\]](#)
- [41] Ge Y, Chen L, Feng H. Ecological optimization of an irreversible Diesel cycle. *Eur Phys J Plus* 2021;136:198. [\[CrossRef\]](#)
- [42] Okumus F, Kokkulunk G, Kaya C, Aydın Z. Thermodynamic assessment of water diesel emulsified fuel usage in a single cylinder diesel engine. *Energy Sources A Recovery Util Environ Eff* 2023;45:3708–3721. [\[CrossRef\]](#)
- [43] Ust Y, Sahin B, Sogut OS. Performance analysis and optimization of an irreversible dual-cycle based on an ecological coefficient of performance criterion. *Appl Energy* 2005;82:23–39. [\[CrossRef\]](#)
- [44] Gonca G, Sahin B. Performance optimization of an air-standard irreversible dual-atkinson cycle engine based on the ecological coefficient of performance criterion. *Sci World J* 2014;2014:e815787. [\[CrossRef\]](#)
- [45] Chandramouli R, Ravi Kiran Sastry G, Gugulothu SK, Srinivasa Rao MSS. Multi-objective optimization of thermo-ecological criteria-based performance parameters of reheat and regenerative braysson cycle. *J Energy Resour Technol* 2021;143:072106. [\[CrossRef\]](#)
- [46] Guo X, Zhang H, Hu Z, Hou S, Ni M, Liao T. Energetic, exergetic and ecological evaluations of a hybrid system based on a phosphoric acid fuel cell and an organic Rankine cycle. *Energy* 2021;217:119365. [\[CrossRef\]](#)
- [47] Ahmadi MH. Thermo-environmental analysis and multi-objective optimization of performance of ericsson engine implementing an evolutionary algorithm. *J Therm Eng* 2019;5:319–340. [\[CrossRef\]](#)
- [48] Ust Y, Sahin B, Kodal A, Akcay IH. Ecological coefficient of performance analysis and optimization of an irreversible regenerative-Brayton heat engine. *Appl Energy* 2006;83:558–572. [\[CrossRef\]](#)
- [49] Ust Y, Sogut OS, Sahin B, Durmayaz A. Ecological coefficient of performance (ECOP) optimization for an irreversible Brayton heat engine with variable-temperature thermal reservoirs. *J Energy Inst* 2006;79:47–52. [\[CrossRef\]](#)
- [50] Sogut OS, Ust Y, Sahin B. The effects of intercooling and regeneration on the thermo-ecological performance analysis of an irreversible-closed Brayton heat engine with variable-temperature thermal reservoirs. *J Phys Appl Phys* 2006;39:4713. [\[CrossRef\]](#)
- [51] Yeginer Y, Kenc S, Komurgoz G, Ozkol I. Ecological performance analysis of irreversible brayton cycle. In: Dincer I, Midilli A, Kucuk H, editors. *Progress in Exergy, Energy, and the Environment*. 1st ed. Berlin: Springer; 2014. pp. 741–749. [\[CrossRef\]](#)
- [52] Sadatsakkak SA, Ahmadi MH, Ahmadi MA. Thermodynamic and thermo-economic analysis and optimization of an irreversible regenerative closed Brayton cycle. *Energy Convers Manag* 2015;94:124–129. [\[CrossRef\]](#)
- [53] Ust Y, Sahin B, Cakir M. Ecological coefficient of performance analysis and optimisation of gas turbines by using exergy analysis approach. *Int J Exergy* 2016;21:39. [\[CrossRef\]](#)
- [54] Ust Y, Sahin B. Performance optimization of irreversible refrigerators based on a new thermo-ecological criterion. *Int J Refrig* 2007;30:527–534. [\[CrossRef\]](#)
- [55] Ust Y. Performance analysis and optimization of irreversible air refrigeration cycles based on ecological coefficient of performance criterion. *Appl Therm Eng* 2009;29:47–55. [\[CrossRef\]](#)
- [56] Ngouateu Wouagfack PA, Tchinda R. Performance optimization of three-heat-source irreversible refrigerators based on a new thermo-ecological criterion. *Int J Refrig* 2011;34:1008–1015. [\[CrossRef\]](#)
- [57] Ngouateu Wouagfack PA, Tchinda R. Optimal performance of an absorption refrigerator based on maximum ECOP. *Int J Refrig* 2014;40:404–415. [\[CrossRef\]](#)
- [58] Gonca G, Ozsari I. Exergetic performance analysis of a gas turbine with two intercoolers and two reheaters fuelled with different fuel kinds. *Proceedings of the ICE - Energy*. 2007;124. [\[CrossRef\]](#)
- [59] Ust Y, Ozsari I. Exergetic performance analysis to compare of two different oxy fuel combustion power plants In: editor. *5th International Conference On Engineering And Natural Science (ICENS'19)*; 2019 June 12-16; Prague, Czech Republic: Zenith Group; 2019. pp.1–12.
- [60] Ust Y, Ozsari I, Arslan F, Safa, Aykut. A theoretical performance investigation of irreversible internal combustion engine named as dual-miller cycle. *Sigma J Eng Nat Sci* 2020;38:459–473.
- [61] Ngouateu Wouagfack PA, Tchinda R. The new thermo-ecological performance optimization of an irreversible three-heat-source absorption heat pump. *Int J Refrig* 2012;35:79–87. [\[CrossRef\]](#)
- [62] Ngouateu Wouagfack PA, Tchinda R. Optimal ecological performance of a four-temperature-level absorption heat pump. *Int J Therm Sci* 2012;54:209–219. [\[CrossRef\]](#)

- [63] Ahmadi MH, Ahmadi MA, Mehrpooya M, Sameti M. Thermo-ecological analysis and optimization performance of an irreversible three-heat-source absorption heat pump. *Energy Convers Manag* 2015;90:175–183. [\[CrossRef\]](#)
- [64] Gonca G. Application of a novel thermo-ecological performance criterion: Effective ecological power density (EFECPOD) to a joule-brayton cycle (JBC) turbine. *J Therm Eng* 2017;3:1478–1488. [\[CrossRef\]](#)
- [65] Gonca G. Exergetic and ecological performance analyses of a gas turbine system with two intercoolers and two re-heaters. *Energy* 2017;124:579–588. [\[CrossRef\]](#)
- [66] Gonca G, Sahin B. Thermo-ecological performance analysis of a Joule-Brayton cycle (JBC) turbine with considerations of heat transfer losses and temperature-dependent specific heats. *Energy Convers Manag* 2017;138:97–105. [\[CrossRef\]](#)
- [67] Fawal S, Kodal A. Comparative performance analysis of various optimization functions for an irreversible Brayton cycle applicable to turbojet engines. *Energy Convers Manag* 2019;199:111976. [\[CrossRef\]](#)
- [68] Gonca G, Başhan V. Multi-criteria performance optimization and analysis of a gas-steam combined power system. *J Braz Soc Mech Sci Eng* 2019;41:373. [\[CrossRef\]](#)
- [69] Gonca G, Genç I. Thermoecology-based performance simulation of a Gas-Mercury-Steam power generation system (GMSPGS). *Energy Convers Manag* 2019;189:91–104. [\[CrossRef\]](#)
- [70] Zerom MS, Gonca G. Multi-criteria performance analysis of dual miller cycle - Organic rankine cycle combined power plant. *Energy Convers Manag* 2020;221:113121. [\[CrossRef\]](#)
- [71] Raman R, Kumar N. Performance analysis of diesel cycle under efficient power density condition with variable specific heat of working fluid. *J Non-Equilib Thermodyn* 2019;44:405–416. [\[CrossRef\]](#)
- [72] Karakurt AS. A New Method for the size and performance optimization of thermal systems: The exergy density. PhD Thesis. Istanbul, Turkiye: Yıldız Technical University; 2018.
- [73] Karakurt AS, Sahin B. Performance analysis and optimization of power cycles via the mean cycle pressure criterion (MCP) and entropy generation (EG). In: Teixeira JC editor. *The 31th International Conference on Efficiency, Cost, Optimization, Simulation and Environmental Impact of Energy Systems*; 2018 June 17-21; Guimaraes, Portugal: University of Minho; 2018.
- [74] Karakurt AS, Sahin B. Performance analyses and optimisation of the Joule-Brayton cycle via the mean cycle pressure criterion. *Int J Exergy* 2018;25:339. [\[CrossRef\]](#)
- [75] Demirbas A. *Methane gas hydrate*. 1st ed. London: Springer; 2010. [\[CrossRef\]](#)
- [76] Netherlands Enterprise Agency. *Gas Composition Transition Agency Report*. Agentschap NL: Ministerie van Economische Zaken; 2013.
- [77] Lefebvre AH, Ballal DR. *Gas turbine combustion alternative fuels and emissions*. 3rd ed. UK: Taylor & Francis; 2010. [\[CrossRef\]](#)
- [78] Lieuwen TC, Yang V. *Gas turbine emissions*. 1st ed. Cambridge: Cambridge University Press; 2013. [\[CrossRef\]](#)
- [79] Richards GA. *New Developments in Combustion Technology-Part II: Step Change in Efficiency*. National Energy Technology Laboratory, 2012.
- [80] Ferguson CR. *Internal combustion engines - applied thermosciences*. 1st ed. New York: John Wiley&Sons Inc; 1986.
- [81] Ozsari I, Ust Y. Effect of varying fuel types on oxy-combustion performance. *Int J Energy Res* 2019;43:8684–8696. [\[CrossRef\]](#)
- [82] Ozsari I, Ust Y, Kayadelen HK. Comparative energy and emission analysis of oxy-combustion and conventional air combustion. *Arab J Sci Eng* 2021;46:2477–2492. [\[CrossRef\]](#)
- [83] Ozsari I, Ust Y. Energy, economic and environmental analysis and comparison of the novel Oxy-combustion power systems. *J Therm Eng* 2022:719–733. [\[CrossRef\]](#)
- [84] Turns SR. *An introduction to combustion: concepts and applications*. 3th ed. Boston: McGraw-Hill; 2011.